Showa Univ J Med Sci **22**(4), 211～219, December 2010

Original

Histological Study of the Left Atrial Wall —A Consideration of the Compound Myocardial Architecture and Potential Durability with Respect to Catheter Ablation in Pulmonary Vein Isolation Procedures—

Genyo OGAWA[1], Shin INOUE[2], Taka-aki MATSUYAMA[3], Mutsuki MAKINO[3], Tetsuo SAKAI[4], Tsukasa SAITO[4], Yoichi KOBAYASHI[4] and Hidekazu OTA[3]

Abstract : Pulmonary vein isolation using radiofrequency energy is performed extensively to treat symptomatic, drug-refractory atrial fibrillation. However, anatomical knowledge of the left atrial wall surrounding the pulmonary vein (PV) openings is insufficient to create an ablation line. Using autopsy hearts from 23 individuals (median age of 63 years), we studied the histological nature of anatomical obstacles or related isthmuses near the PV openings. None of the individuals had a history of tachyarrhythmia or other major cardiac abnormalities. After macroscopic measurement of the minimum width of each isthmus, the following areas were excised and histologically prepared: atrial roof-mitral valve annulus (MVA), left superior pulmonary vein (LSPV) -left atrial appendage (LAA), LAA-MVA, left inferior pulmonary vein (LIPV) -MVA, right superior pulmonary vein (RSPV)-fossa ovalis (FO), right inferior pulmonary vein (RIPV)-FO, and FO-MVA. Within the obstacles near the PV openings, the LSPV-LAA isthmus was found to be the narrowest, whereas the LIPV-MVA was the widest and thickest isthmus. Histological complexity of each isthmus was determined, and the compound architecture of the myocardium was revealed. The further presence of a variety of nerve endings as well as myocardial blood supply enhanced the tissue diversity. Such an insight into the diversity of myocardial architecture or histological complexity in each isthmus might be helpful in creating a reliable ablation line in pulmonary vein isolation procedures.

Key words : left atrium, anatomical obstacles, catheter ablation, isthmus, pulmonary vein

[1] *Department of Internal Medicine, Showa University Toyosu Hospital*, 4-1-18 Toyosu, Koto-ku, Tokyo 135-8577, Japan.
[2] *Department of General Internal Medicine, Showa University Dental Hospital.*
[3] *Second Department of Pathology, Showa University.*
[4] *Division of Cardiology, Department of Medicine, Showa University.*

Introduction

Approximately 90% of atrial ectopies that trigger atrial fibrillation (AF) are derived from myocardial sleeves of the pulmonary vein (PV) openings. PV isolation using radiofrequency energy has therefore been introduced to treat drug-resistant, symptomatic atrial fibrillation[1]. Despite advances in ablation procedures, the recurrence rate of AF after PV isolation remains considerably high[2]. One possible mechanism underlying the recurrence may be the reconnection of ablated atrial musculature surrounding the PV openings[3]. In addition to the technical challenges, the tissue architecture of the left atrium may be involved in ablation line reconnection[4]. To create a reliable ablation line in the PV isolation procedure, it is crucial to understand the detailed myocardial anatomy around the PV openings. We explored the tissue architecture of each isthmus encircling the PV openings with special attention to thoracic veins (coronary sinus and Marshall oblique vein) and interatrial musculature in human autopsy hearts.

Methods

Specimens were from 23 autopsy hearts of 17 women and 6 men (mean age, 63 years; range, 33–81 years). Causes of death were malignancy in 17 cases, and respiratory disease, cerebrovascular disease, and liver disease in 2 cases each. No history of tachyarrhythmia was noted in any of the individuals and death was not caused by cardiovascular disease.

After formalin fixation, the shortest distance between the PV openings and anatomical obstacles was measured to determine the width of the isthmus. To measure the distance between the PV opening and obstacles, we designated the starting point of a sink or protrusion from a level atrial wall as the anatomical border. Since the fossa ovalis margin was not clear from the left atrial aspect, we employed lighting from the back as shown in Fig. 2, followed by removal of the primary atrial septum flap valve for precise measurement.

The measurement was done from point-to-point as follows: the left atrial roof and mitral valve annulus (MVA), left superior pulmonary vein (LSPV) and left atrial appendage (LAA), LAA and MVA, left inferior pulmonary vein (LIPV) and MVA, right superior pulmonary vein (RSPV) and fossa ovalis (FO), right inferior pulmonary vein (RIPV) and FO, and FO and MVA. After measurements were taken, a tissue sample from each site was removed and embedded in paraffin for histological investigation. After Azan-Mallory staining, we observed the myocardial architecture in each sample under the microscope. Additionally, we measured the maximal thickness of the musculature comprising each isthmus.

Results

The mean heart weight was 375 g, ranging from 270 to 470 g. In the left PV openings, a common antrum was observed in 3 out of the 23 hearts studied. Although there were no specimens with a common antrum in the right PV openings, a right middle PV opening

Table 1 The mean width of each isthmus

LSPV-LAA	8.4 mm (5.5 ～ 22.0)
LAA-MVA	12.0 mm (8.4 ～ 17.8)
LIPV-MVA	29.3 mm (15.0 ～ 46.8)
RSPV-FO	24.7 mm (15.8 ～ 33.2)
RIPV-FO	17.2 mm (12.2 ～ 24.0)
FO-MVA	19.4 mm (12.0 ～ 25.0)

Table 2 The mean maximal wall thickness of isthmus and roof

LSPV-LAA	4.0 mm (2.2 ～ 6)
LAA-MVA	3.7 mm (2.5 ～ 6.5)
LIPV-MV	4.5 mm (3.2 ～ 8)
RSPV-FO	3.3 mm (2 ～ 5.5)
RIPV-FO	3.4 mm (2 ～ 5)
FO-MVA	4.0 mm (2.5 ～ 7)
ROOF	5.9 mm (3 ～ 11)

was observed in 3 hearts. Table 1 details the measurements of the width of each isthmus. The widest isthmus was LIPV-MVA, with a mean length of 29.3 mm and range of 15.0 to 46.8 mm. Individual differences are marked, and maximum and minimum values differed almost threefold. The narrowest isthmus was LSPV-LAA with a mean width of 8.4 mm. Minimum and maximum measurements in this isthmus varied four fold, ranging from 5.5 to 22.0 mm. In every isthmus, the values were highly variable, and there was no correlation between isthmus measurements and age, gender, or heart weight.

Table 2 lists the mean maximal thickness of the left atrial wall. The atrial roof was the thickest, with a mean of 5.9 mm and range of 3.0 to 11.0 mm. LIPV-MVA was the second largest, with a mean of 4.5 mm and range of 3.2 to 8.0 mm. Even in the thickest part of the left atrium, each value was highly diverse, and there was no correlation of thickness with age, gender, or heart weight.

Composite photographs in Fig. 1 show measurements around the LSPV or LIPV and LAA. The upper left panel shows a macroscopic overview of the lateral wall of the left atrium with a long-axis cross-section. The heart was sliced from the midline of the posterior left atrium wall to the apex. Based on endocardial images, the left atrium appears relatively flat except for the pectinate muscle within the LAA. Within the LIPV-MVA, however, crevices (or pectinate muscle-like structures) were found in 6 hearts (asterisk). Three double-headed arrows represent 3 isthmuses, each shown in 3 additional photomicrographs. LSPV-LAA (a) represents the histology from a short-axis view. The double-headed arrow indicates the isthmus width. The right lower portion is the pectinate muscle of the LAA, and the left terminal portion is the muscular sleeve of the LSPV. Within the adipose

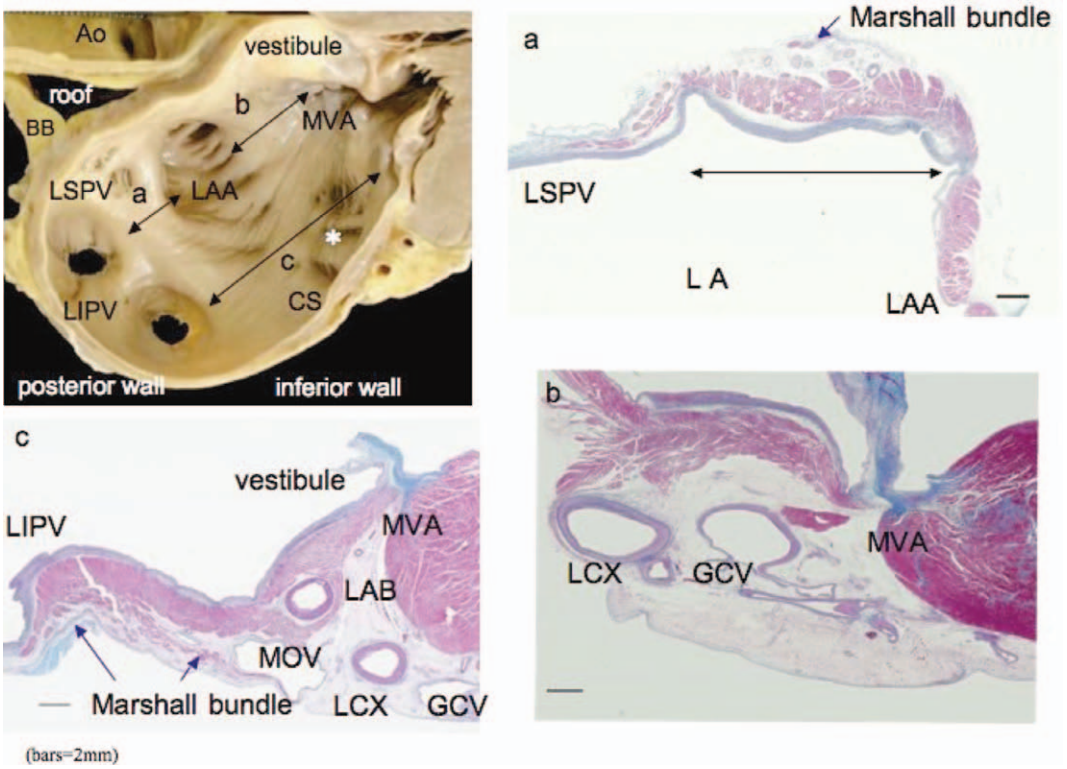

Fig. 1. Isthmuses around the left pulmonary vein openings and left atrial appendage
Within the macroscopic overview of the left atrium (upper left), isthmuses comprised of (a) left superior pulmonary vein (LSPV)- left atrial appendage (LAA), (b) LAA- mitral valve annulus (MVA), and (c) left inferior pulmonary vein (LIPV)- MVA are depicted. Additional photomicrographs represent histological findings of each isthmus, respectively. Ao = aortic root, BB = Bachmann's bundle, CS = coronary sinus, GCV = great cardiac vein, LA left atrium, LAB = left atrial branch, LCX = left circum flex artery, MOV = oblique vein of Marshall, * = crevices. 78-year-old male, bar = 2 mm, Azan-Mallory stain.

tissue, abundant nerve tissues that are presumably sympathetic fibers were observed in all heart specimens, and a Marshall Bundle was observed in one heart[5-7]. LAA-MVA shown in (b) ranged from 8.4 to 17.8 mm, with an average of 12.0 mm, and a mean maximal thickness ranging from 2.5 to 6.5 mm, with an average of 3.7 mm. Because this area presumably represented the mitral vestibule, tissue differences appeared at a relatively low rate. However, it should be noted that the vestibule is comprised of the atrioventricular ring tissue and potentially retains nodal characteristics, as shown in Fig. 3. In the LIPV-MVA (c), the Marshall bundle (i.e., myocardial sleeve) around the Marshall oblique vein (MOV) was broadly spread from the great cardiac vein (GCV) to the LIPV opening. In this isthmus, the MOV and Marshall bundle were found in 13 hearts. In this case, the left atrial branch of the left circumflex artery penetrated the vestibule myocardium.

Fig. 2 is a composite photograph showing a macroscopic overview of the left atrium septal surface (upper left) and additional photomicrographs of three isthmuses, indicated

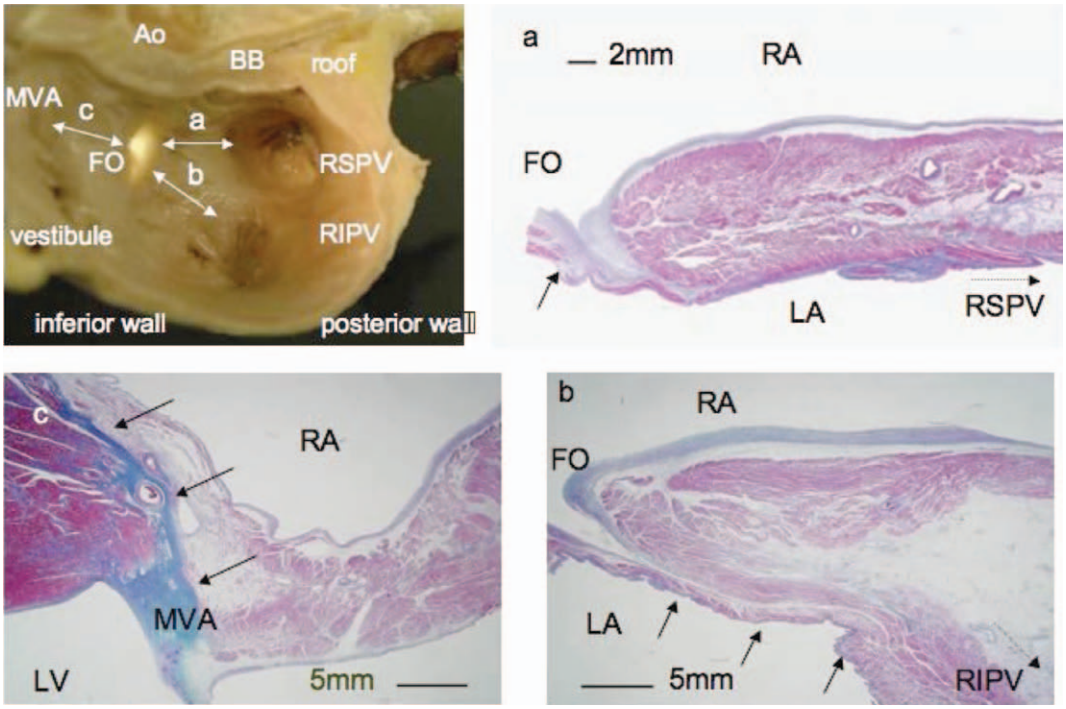

Fig. 2. Isthmuses around the right pulmonary vein openings and foramen ovale
Macroscopic overview (upper left) indicates isthmuses comprised of (a) right superior pulmonary vein (RSPV)-fossa ovalis (FO), (b) right inferior pulmonary vein (RIPV)-FO, and (c) FO-mitral valve annulus (MVA). Additional photomicrographs show compound histological architecture in each isthmus, respectively. Ao = aortic root, BB = Bachmann's bundle, LA = left atrium, RA = right atrium. 78-year-old male, Azan-Mallory stain.

by double-headed arrows (a–c). The width of the RSPV-FO isthmus was 15.8–33.2 mm, with a mean of 24.7 mm, and its trans-septal thickness was 2.0–5.5 mm, with a mean of 3.3 mm. The RIPV-FO isthmus width was 12.2–24.0 mm, with an average of 17.2 mm (trans-septal thickness, 2.0–5.0 mm, mean of 3.4 mm). The FO-MVA distance was 12.0–25.0 mm, with a mean of 19.4 mm (trans-septal thickness, 2.5–7.0 mm, mean of 4.0 mm). Additional photomicrographs (a) showed RSPV-FO. Note the layered musculature comprising the primary atrial septum (arrow) and left and right atrial myocardia. The RIPV-FO isthmus is shown in (b). At this level, the myocardial sleeve of RIPV seems to be continuous with the septum primum (arrows). In the FO-MVA isthmus shown in (c), the muscular part of the atrioventricular septum harbors nodal tissue adjacent to the MVA or the central fibrous body (arrows).

Fig. 3 represents a composite overview of the left atrium (lower left) showing the roof (a) and vestibule (b) with double-headed arrows. Additional photomicrographs show the histology of the short axis view of the roof (a) and thickness, including the insertion of Bachmann's bundle (BB) (arrow). Note the laminar appearance and disarray of the myo-

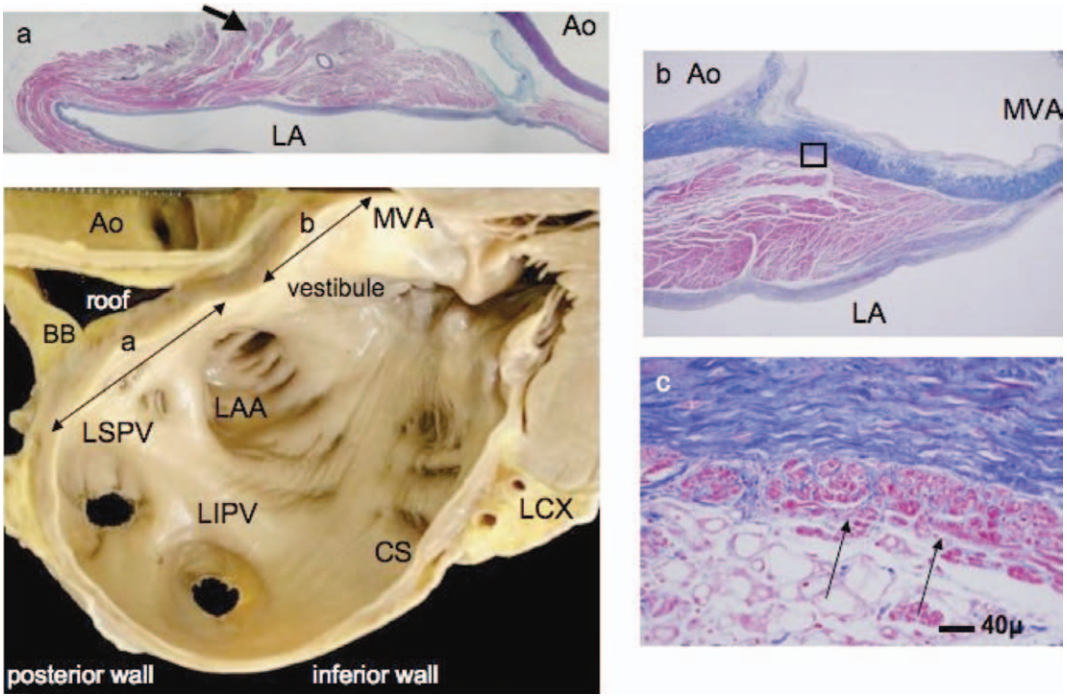

Fig. 3. Histological findings in atrial roof and vestibule
Upper left macroscopic overview indicates (a) area of roof and (b) vestibule.
Additional photomicrographs represent layered architecture of myocardium in this area.
(c) Higher magnification view of rectangular area (boxinb) shows the distribution of specialized conducting tissue (arrows) behind non-coronary cusp. Ao = aortic root, CS = coronary sinus, LA = left atrium, LCX = left circum flex artery, MVA = mitral valve annulus, (a) short arrow = Bachmann's bundle (BB). 51-year-old male, Azan-Mallory stain.

cardium adjacent to the BB. The photomicrograph of the vestibule (b) shows enhancement of tissue heterogeneity represented by increased collagen (shown in blue) within myocardium (shown in red). Within the rectangular area shown by a high power photomicrograph (c), nodal tissue (arrows) was observed in one heart in this series.

Discussion

Measurements taken in this study of 23 autopsy hearts revealed no correlation between the dimension of each isthmus and heart weight or age. In addition, individual differences in each value were highly diverse. Our morphological analysis of the PV openings showed the common antrum of the left PVs and the middle PV of the right PV in 3 of 23 hearts. These morphological variations are likely to influence the ablation procedure in extensive pulmonary isolation. Particularly, the mid-PV opening may enhance tissue non-uniformity in the carina of right PV openings[3].

Within isthmuses in the left atrium, the LIPV-MVA is established as an additional ablation line (posterior line) in the PV isolation procedure[8]. Despite the prevalence of

this application, however, this isthmus was the widest and thickest, and at the same time, individual differences were highly diverse. Macroscopic examination revealed an irregular pectinate muscle structure in 6 of 23 specimens, and Su *et al*[9] designated these structures as crevices. The crevices make endocardial tissue appear complex, and seem to interfere with the ablation procedure. One factor influencing the ablation line may be the blood vessels in this area, as shown in Figure 1c, because of their cooling effect on radiofrequency energy. The most important structure in this isthmus may be the broad Marshall bundle beneath the epicardium. The Marshall bundle is the remnant of a muscularized sleeve of an embryological left superior caval vein and is thought to have relatively unstable electrophysiological properties[5]. Since endocardial application of radiofrequency energy results in hemisphere tissue injury within the atrial walls[10], complete interruption of the subepicardial Marshall bundle needs a specialized and detailed procedure.

LSPV-LAA is regarded as a crucial area because the ablation line for PV isolation passes through LSPV-LAA[11]. Based on the shape running around the PV openings, the LSPV-LAA isthmus is known as the anterior ridge or fold of the left atrium. Although the LSPV-LAA isthmus is the narrowest, there are considerable individual differences not only in its width but also in thickness. In addition to macroscopic variation, the myocardial architecture, including blood vessels, nerve fibers, and extension of Marshall bundles, enhances tissue non-uniformity. Although our results using autopsy hearts indicated a mean width of 8.4 mm, recent clinical reports by MRI reported the LSPV-LAA as 5.8–6.4 mm[12–14]. Differences in data, particularly shorter dimensions in clinical value, may be attributed to the condition of the atrial cavity, i.e., the tension of atrial wall caused by blood fulfillment may enhance irregularities and sharpen this ridge. Despite advances in MRI and multislice CT technology, detailed myocardial arrangement of CS musculature or Marshall bundle remains unclear. Further histological analysis of human hearts is therefore required to increase the understanding of electro-mechanical architecture in this area.

Microscopic observation of isthmuses between the right PV openings and the FO, muscularized flap valves of FO (remnant of the primary atrial septum), and left and right myocardial components of interatrial grooves revealed a complex morphology (Fig. 2). Interestingly, the myocardium of the flap valve appears continuous with the myocardial sleeve of the right PVs, possibly because these musculatures were originally termed the *septopulmonary bundle* in 1920 by Papes[15].

Compared with other isthmuses, FO-MVA and LAA-MVA have a relatively constant appearance. This phenomenon may be partially explained in that these areas represent the mitral vestibule, including the atrioventricular ring tissue. Occasionally, the mitral annulus attaches remnants of the specialized conducting tissue and evokes re-entrant atrial tachycardia[16].

In contrast to the right atrium, the left atrium epicardial aspects displayed complexity accompanying the supplementary myocardium, such as the coronary sinus musculature, Mar-

shall bundle, and BB[15]. Distribution of these musculatures and their irregularities are likely to influence the outcome of the PV isolation procedure. Immunohistochemical analysis of the cellular diversity within each isthmus including the expression products of epitope genes should be undertaken, in addition to more detailed morphological observation by confocal optical microscopy or scanning electron microscopy, with the aim of revealing novel myocardial architecture.

Limitations

One of the limitations of this study is that only normal heart without tachyarrhythmia was analyzed. In addition, deformation of the atrial wall could probably occur during the fixation process[17], although the focus of this study was the compound architecture of the each isthmus (myocardium, thoracic veins, BB, and interatrial tissue). We could apply these data to clinical studies to evaluate hearts with arrhythmia.

Conclusion

There are considerable individual differences in the dimensions and histological measurements of the left atrial isthmuses. Detailed anatomical knowledge of the left atrium is important for creating a reliable ablation line in PV isolation procedures.

References

1) Haïssaguerre M, Jais P, Shah DC, Takahashi A, Hocini M, Quiniou G, Garrigue S, Le Mouroux A, Le Metayer P and Clementy J : Spontaneous initiation of atrial fibrillation by ectopic beats originating in the pulmonary veins. *N Engl J Med* **339** : 659–666 (1998)
2) Oral H, Pappone C, Chugh A, Good E, Bogun F, Pelosi F Jr, Bastes ER, Lehmann MH, Vicedomini G, Augello G, Agricola E, Sala S, Santinelli V and Morady F : Circumferential pulmonary-vein ablation for chronic atrial fibrillation. *N Engl J Med* **354** : 934–941 (2006)
3) Valles E, Fan R, Roux JF, Harding JD, Dhruvakumar S, Hutchinson MD, Riley M, Bala R, Garcia FC, Lin D, Dixit S, Callans DJ, Gerstenfeld EP and Marchlinski FE : Localization of atrial fibrillation triggers in patients undergoing pulmonary vein isolation : importance of the carina region. *J Am Coll Cardiol* **52** : 1413–1420 (2008)
4) Ho SY and Sanchez-Quintana D : The importance of atrial structure and fibers. *Clin Anat* **22** : 52–63 (2009)
5) van den Hoff MJ, Kruithof BP and Moorman AF : Making more heart muscle. *Bioessays* **26** : 248–261 (2004)
6) Makino M, Inoue S, Matsuyama T, Ogawa G, Sakai T, Kobayashi Y, Katagiri T and Ota H : Diverse myocardial extension and autonomic innervation on ligament of Marshall in humans. *J Cardiovasc Electrophysiol* **17** : 594–599 (2006)
7) Matsuyama T, Inoue S, Kobayashi Y, Makino M, Sakai T, Saito T, Asano T, Tanno K, Katagiri T and Ota H : Arrangement of the autonomic nerves around the pulmonary vein-left atrial junctions : histologic and immunohistochemical analyses. *J Arrhythmia* **22** : 234–241 (2006)
8) Becker AE : Left atrial isthmus : anatomic aspects relevant for linear catheter ablation procedure in humans. *J Cardiovasc Electrophysiol* **15** : 809–814 (2004)
9) Su P, McCarthy KP and Ho SY : Occluding the left atrial appendage : anatomical considerations. *Heart* **94** : 1166–1170 (2008)
10) Tanno K, Kobayashi Y, Kurano K, Kikushima S, Yazawa T, Baba T, Inoue S, Mukai H and Katagiri T : Histopathology of canine heart subjected catheter ablation using radiofrequency energy. *Jpn Circ J* **58** : 123–135

(1994)
11) Ching CK, Patel D and Natale A : Catheter ablation of atrial fibrillation. *J Arrhythmia* **23** : 85-101 (2007)
12) Mansour M, Refaat M, Heist EK, Mela T, Cury R, Holmvang G and Ruskin JN : Three-dimensional anatomy of the left atrium by magnetic resonance angiography : implications for catheter ablation for atrial fibrillation. *J Cardiovasc Electrophysiol* **17** : 719-723 (2006)
13) Schmidt B, Ernst S, Ouyang F, Chun KR, Broemel T, Bansch D, Kuck KH and Antz M : External and endoluminal analysis of left atrial anatomy and the pulmonary veins in three-dimensional reconstructions of magnetic resonance angiography : the full insight from inside. *J Cardiovasc Electrophysiol* **17** : 957-964 (2006)
14) Wongcharoen A, Tsao HM, Wu MH, Tai CT, Chang SL, Lin YJ, Lo LW, Chen YJ, Sheu MH, Chang CY and Chen SA : Morphologic characteristics of the left atrial appendage, roof, and septum : implications for the ablation of atrial fibrillation. *J Cardiovasc Electrophysiol* **17** : 951-956 (2006)
15) Papez JW : Heart musculature of the atria. *Am J Anat* **27** : 255-285 (1920)
16) Matsuyama TA, Inoue S, Tanno K, Makino M, Ogawa G, Sakai T, Kobayashi Y, Katagiri T and Ota H : Ectopic nodal structures in a patient with atrial tachycardia originating from the mitral valve annulus. *Europace* **8** : 977-979 (2006)
17) Docquier PL, Paul L, Cartiaux O, Lecouvet F, Dufrane D, Delloye C and Galant C : Formalin fixation could interfere with the clinical assessment of the tumor-free margin in tumor surgery : magnetic resonance imaging-based study. *Oncology* **78** : 115-124 (2010)

[Received October 5, 2010 : Accepted October 27, 2010]